Natural genetic variation underlying the negative effect of elevated CO2 on ionome composition in Arabidopsis thaliana

Oceane Cassan, Lea-Lou Pimpare, Mozzanino Timothy, Cecile Fizames, Sebastien Devidal, Fabrice Roux, Alexandru Milcu, Sophie Lebre, Alain Gojon, Antoine Martin

Natural genetic variation underlying the negative effect of elevated CO_2 on ionome composition in *Arabidopsis thaliana*

Océane Cassan[1], Léa-Lou Pimparé[1], Timothy Mozzanino[1], Cécile Fizames[1], Sébastien Devidal[2], Fabrice Roux[3], Alexandru Milcu[2,4], Sophie Lèbre[5], Alain Gojon[1], Antoine Martin[1*]

[1] IPSiM, Univ Montpellier, CNRS, INRAE, Institut Agro, 34060, Montpellier, France

[2] Montpellier European Ecotron, Univ Montpellier, CNRS, Campus Baillarguet, 34980, Montferrier-sur-Lez, France

[3] Laboratoire des Interactions Plantes-Microbes-Environnement, Institut National de Recherche pour l'Agriculture, l'Alimentation et l'Environnement, CNRS, Université de Toulouse, Castanet-Tolosan, France

[4] CEFE, Univ Montpellier, CNRS, EPHE, IRD, UPVM, SupAgro, INRAE, 34293, Montpellier, France

[5] IMAG, Montpellier, France

*Author for correspondence: antoine.martin@cnrs.fr

Abstract

The elevation of atmospheric CO_2 leads to a decline in the plant mineral content, which poses a major threat to food security in the coming decades. To date, very few genes have been identified as having a role in the negative effect of elevated CO_2 on plant mineral composition. Yet, several studies have shown a certain degree of diversity in the ionome's response to elevated CO_2, associated with genotypic variation. This suggests the existence of genetic factors controlling the effect of CO_2 on ionome composition. However, no large-scale studies have been carried out to date to explore the genetic diversity of the ionome responses to elevated CO_2. Here, we used six hundred *Arabidopsis thaliana* accessions, representing geographical distributions ranging from worldwide to regional and local environments, to analyze the natural genetic variation underlying the negative effect of elevated CO_2 on the ionome composition in plants. We show that the growth under elevated CO_2 leads to a global and important decrease of the ionome content whatever the geographic distribution of the population. We also observed a high range of genetic diversity in the response of the ionome composition to elevated CO_2, and we identified sub-populations, showing effects on their ionome ranging from the most pronounced to resilience or even to a benefit in response to elevated CO_2. Using genome-wide association mapping on the response of each mineral element to elevated CO_2 or on integrative traits, we identified a large set of QTLs and genes associated with the ionome response to elevated CO_2. Finally, we demonstrate that manipulating the function of one of these genes can mitigate the negative effect of elevated CO_2 on the plant mineral composition. Therefore, this resource will contribute to understand the genetic mechanisms underlying the negative effect of elevated CO_2 on the mineral composition of plants, and to the development of biofortified crops adapted to a high-CO_2 world.

Introduction

The elevation of atmospheric CO_2 concentration leads to a decline in the mineral composition of C3 plants [1]. The negative effect of elevated CO_2 on plant mineral composition has been observed worldwide, and alters the content of nutrients that are essential for human nutrition, such as nitrogen (N) and proteins, iron (Fe) or zinc (Zn) [2]. The rise in atmospheric CO_2 thus poses a major threat to food security in the coming decades. The reasons why elevated CO_2 leads to the degradation of plant mineral composition are far from being well understood. To date, only a few genes with a potential regulatory effect on this mechanism have been identified [3-7]. These elements nevertheless converge towards the fact that the adaptation of plants to future high CO_2 climate can be achieved through the identification and the characterization of genetic mechanisms. In addition to this, several studies suggest that exploring the natural genetic variability of plants represents a major opportunity to understand the mechanisms by which high CO_2 leads to a decline in plant mineral composition [8-10]. Indeed, a significant diversity in the response of mineral composition to high CO_2 has been observed in several plant species. For protein and therefore N content, as well as for Fe or Zn content, substantial variations have been observed between small panels of genotypes from different species [8-10]. This implies the presence of a genetic diversity reservoir, which can facilitate the understanding of the ionome's response to high CO_2 and subsequently provide an opportunity to alleviate this negative impact. However, in order to identify the genetic determinants of this negative response of the ionome to high CO_2, large-scale approaches are necessary, but are still lacking for the moment. The objective of this work was to fill the aforementioned knowledge gap by using a large collection of natural genotypes of the model plant *Arabidopsis thaliana* allowing to explore in depth the natural variation of the ionome response to elevated CO_2, and to generate a resource of phenotypic data that can be used in

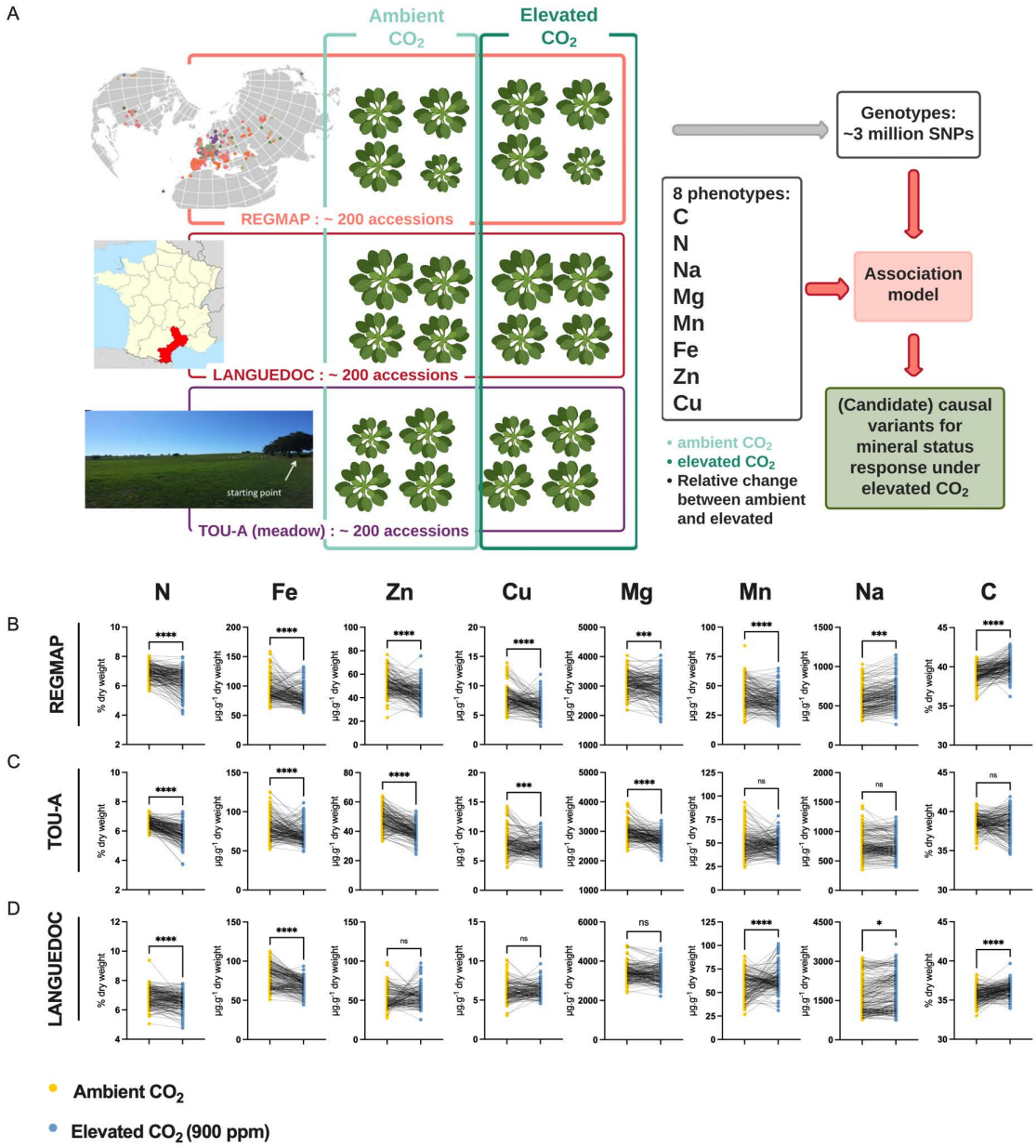

Figure 1: Elevated CO_2 negatively impacts the ionome content at the population-scale level in *Arabidopsis thaliana*. A. Representation of the experimental design used in this study. The content of eight mineral elements was assessed for around 600 *Arabidopsis thaliana* accessions coming from the REGMAP (B), LANGUEDOC (C) and TOU-A (D) populations. Each dot represents the value of the content of a mineral element for one accession (yellow: ambient CO_2 (aCO_2, ~420 ppm), blue: elevated CO_2 (eCO_2, 900 ppm). N (% of dry weight), Fe ($\mu g.g^{-1}$ dry weight), Zn ($\mu g.g^{-1}$ dry weight), Cu ($\mu g.g^{-1}$ dry weight), Mg ($\mu g.g^{-1}$ dry weight), Mn ($\mu g.g^{-1}$ dry weight), Na ($\mu g.g^{-1}$ dry weight), C (% of dry weight). Asterisks indicate significant differences (Paired Wilcoxson test; *, $P<0.05$; **, $P<0.005$; ***, $P<0.0005$). ns; not significant.

association genetics approaches. To this end, we used several hundreds of accessions from different geographic scales of *A. thaliana*, and analyzed their mineral composition under contrasted conditions of CO_2 concentration. This allowed us to extract the general trends in the ionome response to high CO_2, and to identify a large set of genes associated with the variation in the mineral composition of plants in response to high CO_2. By combining this information with genome expression data under elevated CO_2, we end up by functionally validating one of these genes for its importance in the reduction of Zn content under elevated CO_2, and therefore by demonstrating the relevance of this resource for future improvement of plant nutrient content under elevated CO_2.

Results

In order to explore the natural variation and identify its underlying genetic basis associated with the negative effect of elevated CO_2 on plant ionome, we used three populations of *A. thaliana* representing different geographic scales (i.e., the worldwide REGMAP population, the LANGUEDOC regional population and the local TOU-A population from east of France) and displaying different levels of genetic diversity (Fig. 1A). These populations were grown under ambient or elevated CO_2, and we measured in each accession the composition of their ionome in rosettes, including C, N, Na, Fe, Mg, Mn, Zn and Cu content.

Elevated CO_2 globally decreases ionome content at the population level, whatever the geographic scale.

In the three *A. thaliana* populations, we observed a global and important decrease of the ionome content when plants were grown under elevated CO_2 as compared to ambient CO_2. This was particularly the case for N and Fe, for which the decrease in content was very robust and important in each of the population analyzed (Fig. 1B-D). Zn, Cu and Mg content were also

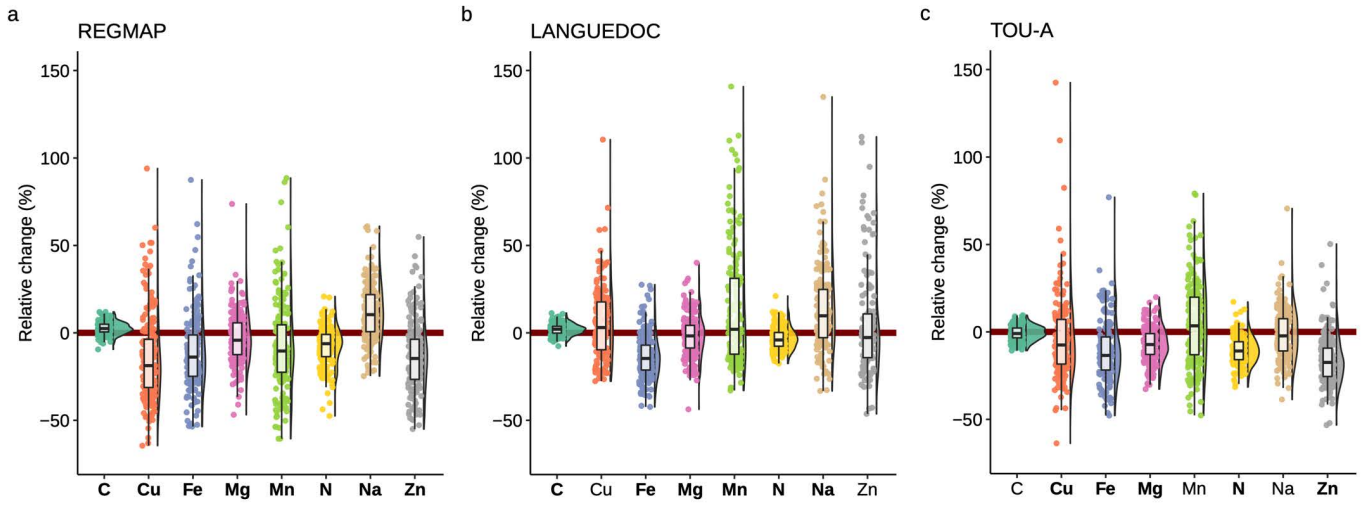

Figure 2: Elevated CO_2 leads to high phenotypic diversity of ionome response in *Arabidopsis thaliana*. Distributions of the relative change (%) of the content of 8 mineral elements between elevated CO_2 and ambient CO_2, in each population (A: REGMAP, B: LANGUEDOC, C: TOU-A). Each dot represents the value of the relative change of the content a mineral element for one accession. The name of the element appears in bold if the mean of the element in elevated CO_2 is significantly different from the mean of the element in ambient CO_2 (Paired wilcoxon test, significance threshold of 0.05).

negatively affected to a significant extent by the growth under elevated CO_2 in the REGMAP and in the TOU-A populations (Fig. 1B, C), although not significantly in the LANGUEDOC population (Fig. 1D). More variability for the effect of elevated CO_2 was observed on Mn and Na content, which were decreased in the REGMAP population, but not significantly changed in the TOU-A and LANGUEDOC populations, respectively. In parallel, the C content of these populations increased under elevated CO_2, by very significant factors for the REGMAP and the LANGUEDOC populations. Altogether, these observations demonstrate that elevated CO_2 has on average a strong negative impact on the mineral content of natural genotypes of *A. thaliana* at the population-scale, whatever their geographic distribution.

The ionome of *Arabidopsis thaliana* natural accessions displays a high range of phenotypic diversity in response to elevated CO_2.

To explore the effect of elevated CO_2 in each accession, we calculated the relative change in nutrient composition of *A. thaliana* accessions from the three populations in response to elevated CO_2. In agreement with the results previously mentioned, we observed that the median relative change of most nutrient content at the population-level was negatively affected by elevated CO_2 (Fig. 2). But the most striking observation was the genetic diversity of ionome response observed in these populations. Indeed, while most the natural accessions were negatively affected by elevated CO_2 (with a negative relative ratio of their nutrient content between ambient and elevated CO_2), a considerable number of accessions were rather not affected by elevated CO_2, or even positively affected, therefore showing an improved nutrient composition under elevated CO_2. For macronutrients like N, the relative change of concentration between ambient and elevated CO_2 varied from 20% to -50%, and for micronutrients like Cu, Fe or Zn, the relative change of concentration between ambient and

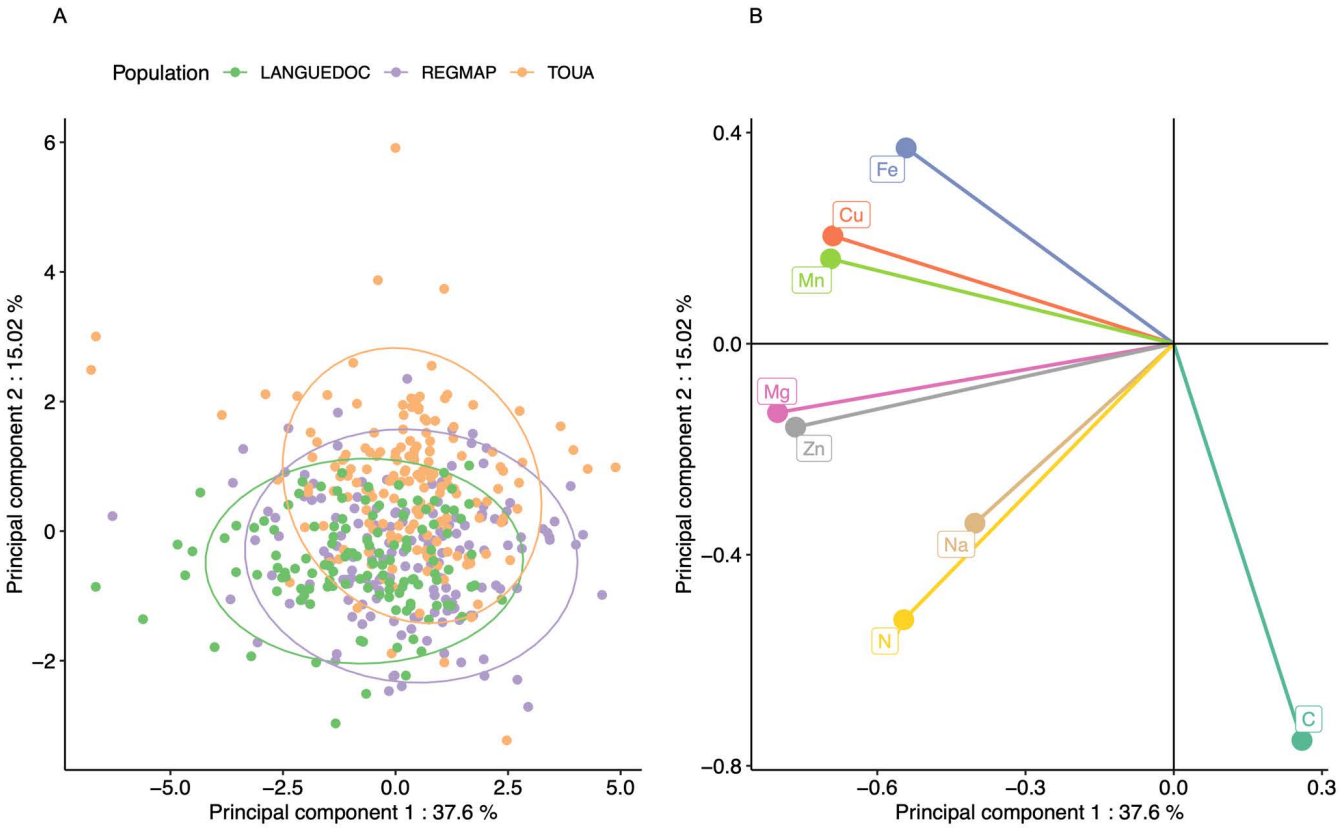

Figure 3: Elevated CO_2 results in a general pattern of ionome variation common to most accessions constituting natural populations of *Arabidopsis thaliana*. Principal Component Analysis (PCA) was performed using the variation of each element in response to elevated CO_2. A. Natural accessions were positioned on the PCA and colored based on population. B. Contribution of each element to the PCA axis.

97 elevated CO_2 varied from 100% to -60% (Fig. 2). In addition, some differences among nutrients
98 were observed between populations. For instance, a smaller dispersion of Fe relative change
99 in the LANGUEDOC population, against a higher distribution of Mn relative change.
100 In order to explore the behavior of the different elements in response to elevated CO_2 and to
101 observe the structure of phenotypic variation, we performed a principal component analysis
102 (PCA) of the relative change in the 8 elements for the accessions from the three populations.
103 The accessions from all populations seem to have globally similar responses to elevated CO_2,
104 as suggested by the overlap of the three populations in the two first principal components
105 (Fig. 3A). The first component of the PCA described a clear antagonistic trend between C
106 content and the change of other mineral elements (Fig. 3B), suggesting that most of the
107 variation between accessions in term of mineral response (almost 40%) could be driven by
108 one or a few mechanisms resulting in an inverse variation between the whole ionome and C
109 change (Fig. 3B). Interestingly, the second component, explaining almost 15% of the variation
110 among accessions in term of mineral response, was mainly driven jointly by change in N and
111 C concentration. Altogether, these results show that there is a marked and large variability
112 among accessions in their mineral concentration in response to elevated CO_2, illustrated by
113 accessions negatively affected by elevated CO_2 and others positively affected by elevated CO_2.
114 In order to explore specific behavior of sub-populations, we clustered the accessions from the
115 REGMAP panel via a k-means approach. This multivariate clustering resulted in the
116 partitioning of accessions in three groups (Fig.4 – Suppl. Table 1). Cluster 1 displayed the most
117 negative pattern of ionome response to elevated CO_2. Inversely, accessions included in Cluster
118 2 displayed a globally positive response, with the highest relative change for almost all mineral
119 elements, except for C content. These accessions did not appear to be clustered
120 geographically with respect to their collection origin in the REGMAP panel (Suppl. Fig. 1),

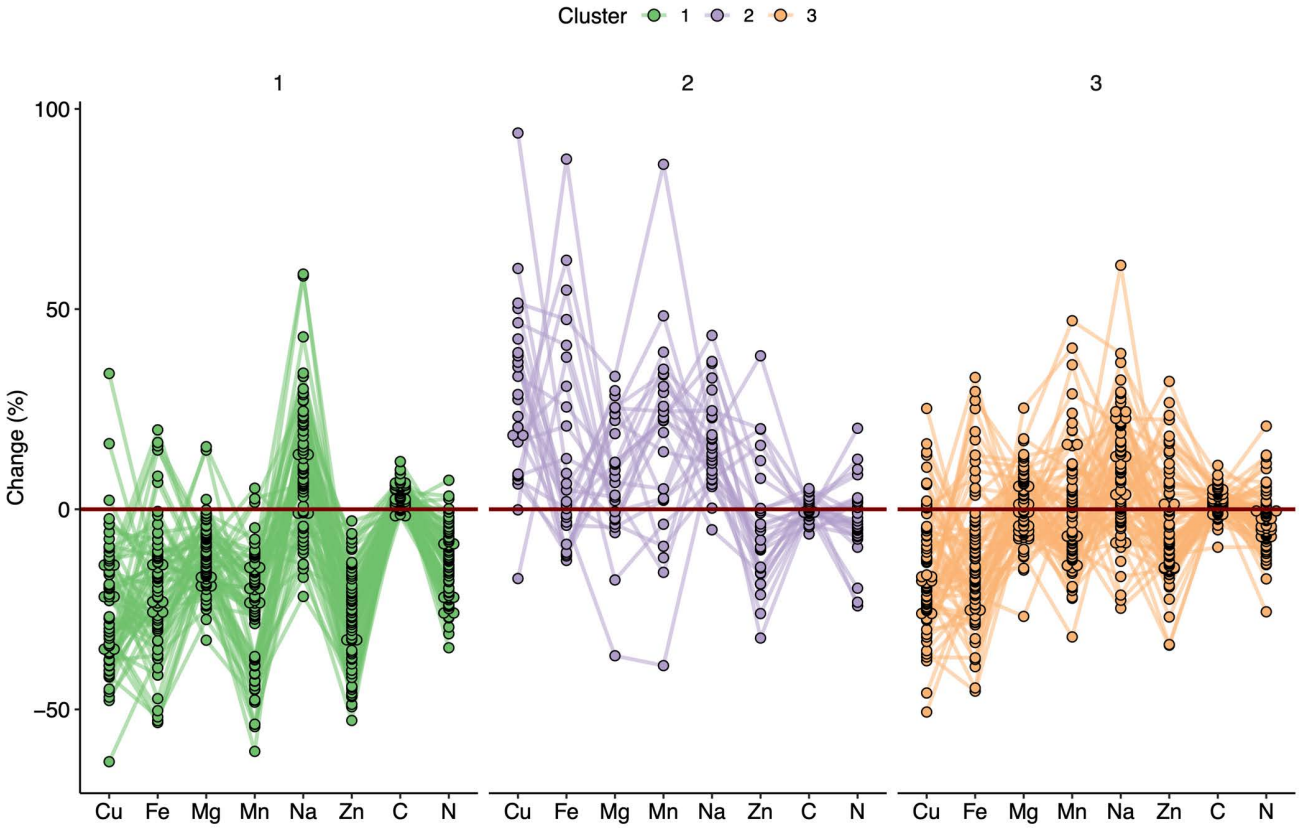

Figure 4: Variation in the response of the ionome to elevated CO_2 identifies contrasting subpopulations inside the REGMAP panel. K-means clustering was performed in the REGMAP accessions to identify different subpopulations. Each accession is represented by a dot, connected by a line between each element. Cluster 1:65 accessions. Cluster 2: 25 accessions. Cluster 3: 69 accessions.

which is in line with the high genetic diversity of response to elevated CO_2 observed at smaller geographical scales (Fig.2). Finally, Cluster 3 displayed a resilient pattern, with accessions showing a globally attenuated response to elevated CO_2. Interestingly, the large phenotypic diversity of the ionome observed in the three populations in response to high CO_2, as well as the presence of contrasted subpopulations in the REGMPA panel, suggests the presence of genetic determinants associated with this response.

Genetic architecture of the ionome response to elevated CO_2, and identification of genetic determinants

We run Genome-Wide Association (GWA) mapping to describe the genetic architecture of the ionome response to elevated CO_2, and to fine-map candidate genes underlying the detected quantitative trait loci (QTLs). We focused here on the phenotypic data collected on the REGMAP population, and used the sequencing data available for this population [11]. We included in this analysis the level of each mineral under ambient and under elevated CO_2, as well as the relative change between ambient and elevated CO_2 for each element. We also included a trait corresponding for each accession to the coordinate on the first and on the second PCA axes (PCA1 and PCA2) explaining collectively more than 50% of ionomic variation (Fig. 3). Therefore, these values correspond to traits driving and summarizing a large part of the ionome variation under elevated CO_2. This resulted as a whole in running GWA mapping on 30 different single-trait GWAS. The overall approach was first validated by observing expected results for traits phenotyped under ambient CO_2. For instance, we observed a very strong peak for the Na content at the locus of the *HKT1* gene (Suppl. Fig. 2A), which is known to be involved in the natural genetic variation of Na content in *Arabidopsis thaliana* [12], or a strong peak for the N content at the locus of the *NIA1* gene (Suppl. Fig. 2B), encoding for an

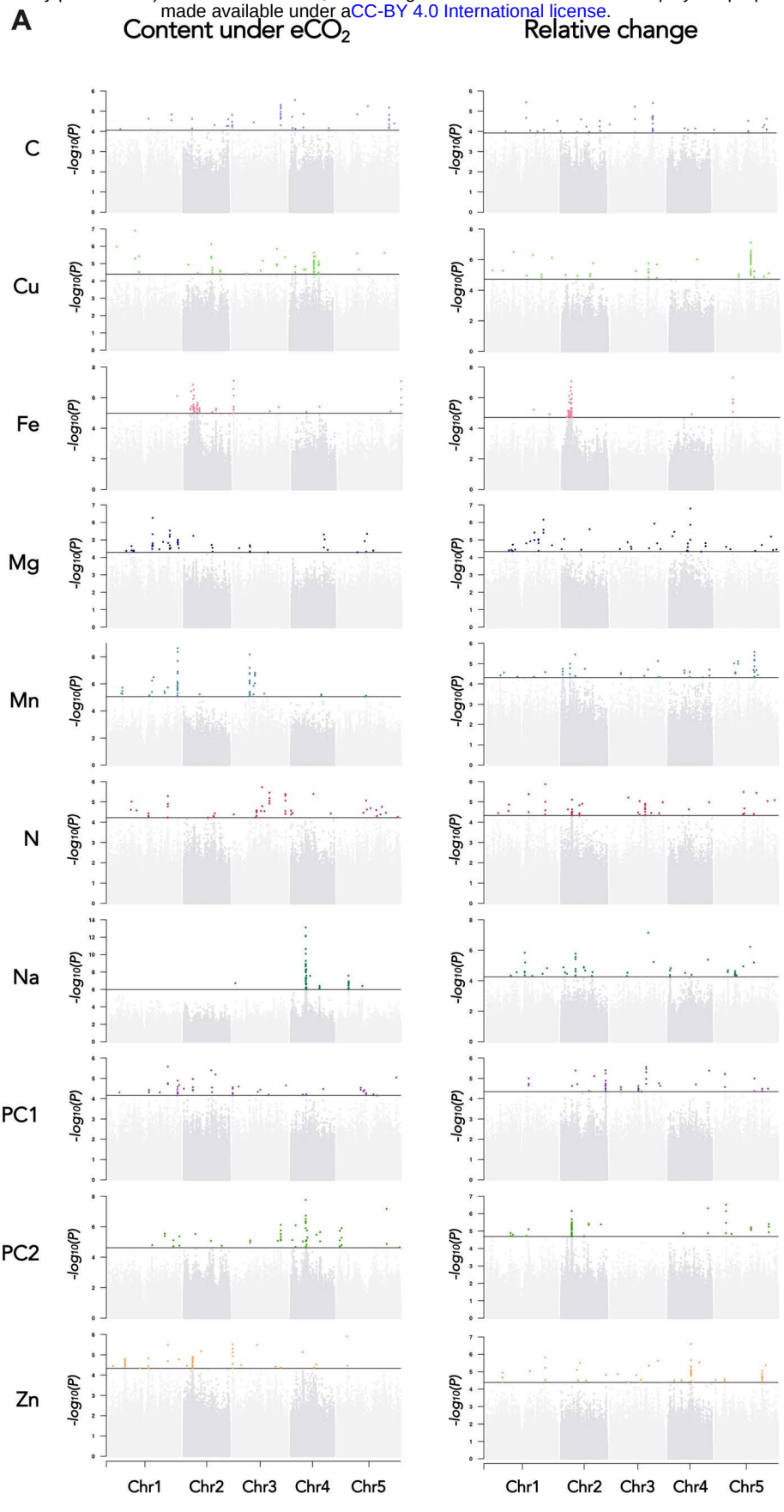

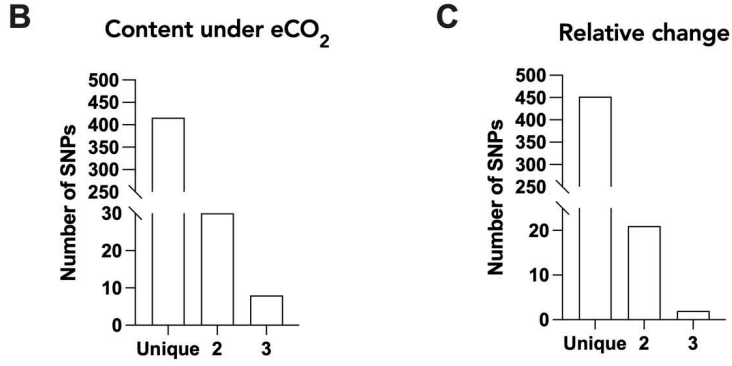

Figure 5: Genetic architecture of the response of the ionome to elevated CO_2 in the REGMAP panel of *Arabidopsis thaliana*. A. Manhattan plots for the content of eight mineral elements under elevated CO_2, or for the relative change of the content of mineral elements between elevated CO_2 and ambient CO_2. For each Manhattan plot, SNPs with the 50 most significant P-value, located above the horizontal line, are colored. Bar plots showing the number of SNPs identified by GWAs for traits under elevated CO_2 (B) or for the relative change of the content of mineral elements between elevated CO_2 and ambient CO_2 (C) that are unique to one element or shared between 2 or 3 traits.

isoform of the nitrate reductase required for the first step of nitrate reduction and associated with natural genetic variation of N content in *A. thaliana* [13].

GWA mapping revealed a polygenic architecture for each phenotypic trait, although its complexity largely differs among traits. For instance, very few and neat peaks of association were detected Na and Mn content under elevated CO2, or of Fe and Cu relative change between ambient and elevated CO2 (Fig.5A, Suppl. Fig. 3). On the other hand, a more complex genetic architecture with the detection of a large number of QTLs was observed for traits related to N or C content (Fig.5A, Suppl. Fig. 3). For each of the traits that have been analyzed under elevated CO_2 or corresponding to the relative change of their content between ambient and elevated CO_2, we isolated the 50 SNPs with the most significant p-value, hereafter named top SNPs (Fig. 5A, Suppl. Tables 2 and 3). In order to identify the overlap between the genetic architecture of each trait, we looked whether some of the top SNPs were shared among traits. While the large majority of SNPs were specific to one trait, 30 and 21 SNPs were shared between two traits for the content under elevated CO_2 or for the relative change between ambient and elevated CO_2, respectively (Fig. 5B and C, Supplemental Tables 2 and 3). In addition, 8 and 2 SNPs were shared between three traits for the content under elevated CO_2 or for the relative change between ambient and elevated CO_2, respectively (Fig. 5B and C, Supplemental Tables 2 and 3). Most of the shared SNPs were associated with micronutrients (Fe, Mn, Zn and Mg content) and with N and/or with the first component of the PCA axis. An interesting QTL located on chromosome 1 was notably associated with 6 traits, displaying SNPs shared between Mn, Zn and N relative change and SNPs shared between Mn, N and PC1 content under elevated CO_2 (Fig. 5A, Suppl. Tables 2 and 3). Another QTL located on chromosome 3 encompasses SNPs shared between Fe, Zn and PC1 content under elevated CO_2 (Fig. 5A, Suppl. Table 2).

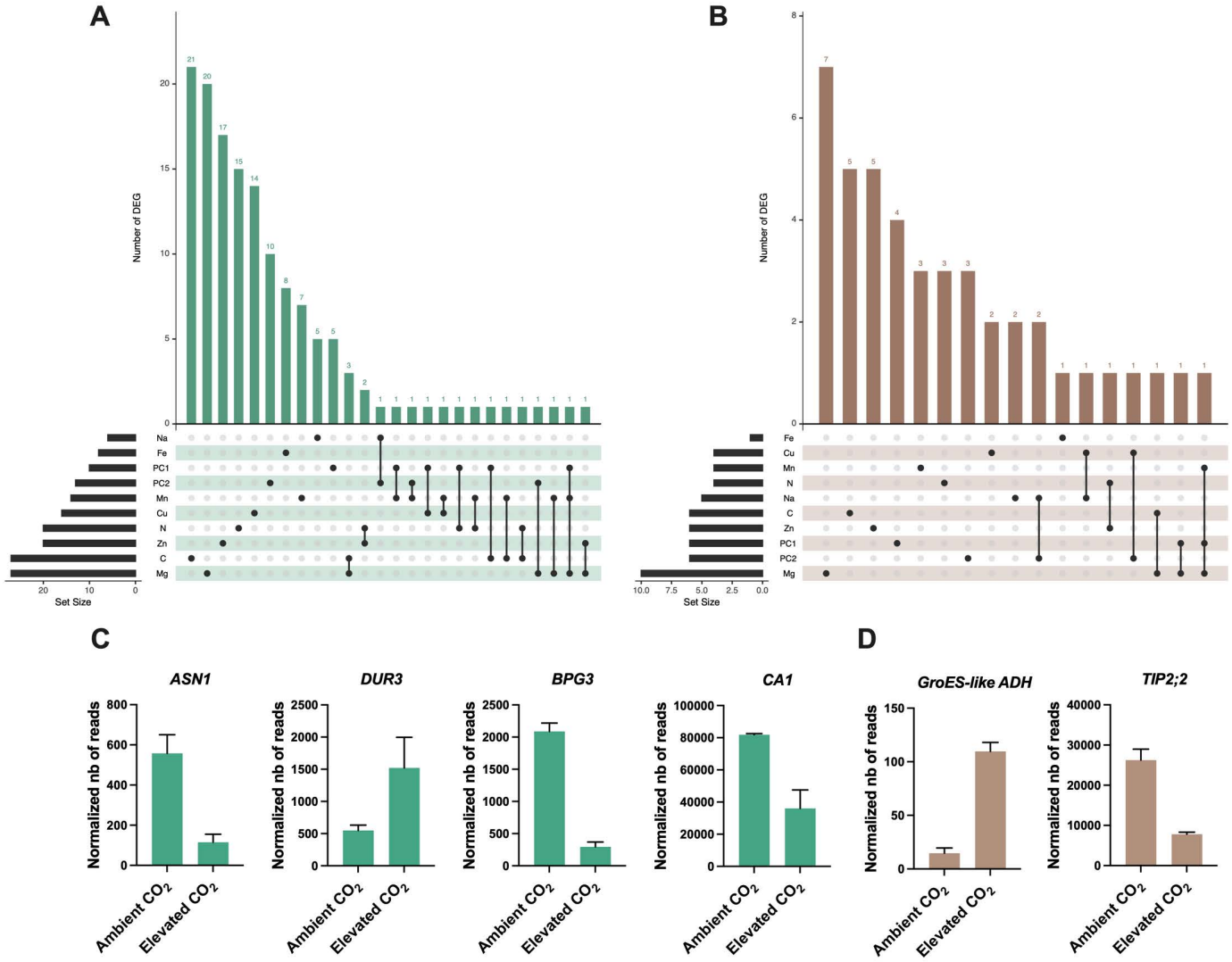

Figure 6: Identification of genes detected by GWA mapping and differentially regulated by elevated CO_2. Intersection between elevated CO_2-DEG in shoot (A) or root (B) and genes identified by GWA mapping. UpSet plots display the number of elevated CO_2-DEG that are associated to a locus identified for the content or the relative change of one or several mineral elements under elevated CO_2. Illustration of the pattern of elevated CO_2-DEG in shoot (C) or root (D) also identified by GWA mapping.

We next identified for each trait a list of the genes located at ±25 kb from the top 50 SNPs, which corresponds to the rough estimate of the decay of linkage disequilibrium identified in *A. thaliana* at the worldwide scale [14]. This resulted in a list of genes for each element, ranging from 154 to 422 genes depending on the element (Suppl. Tables 2 and 3). Among others, several genes associated with top 50 SNPs were identified as obvious candidates of the effect of elevated CO_2 on plant nutrition and ionome content. This was the case of *ZINC INDUCED FACILITATOR 1* (*ZIF1*, *AT5G13740*) and *ZIF-LIKE1* (*AT5G13750*), linked with SNPs identified for Zn content under elevated CO_2, and involved Zn sequestration mechanisms [15]. We also noticed the link between SNPs identified for Zn relative change and *TIP2;2* (*AT4G17340*), known to be involved in Zn root-to-shoot translocation [16]. Concerning N relative change, some of the top 50 SNPs were linked to *ASN1* (*AT3G47340*), which is an actor of N status and remobilization [17,18]. The *H+/CATION EXCHANGER 1* (*CAX1*) gene (*AT2G38170*), involved in the response to Mn deficiency, was also linked to SNPs associated with Mn content under elevated CO_2 [19]. Some of the top 50 SNPs identified for Fe relative change were linked to *MCO2* (*AT5G21100*) and *MCO3* (*AT5G21105*) genes, which have been recently characterized as actors of the regulation of Fe homeostasis [20]. Finally, it is interesting to note that the QTL located on chromosome 3 mentioned above displaying significant shared SNPs identified for Fe, Zn and PC1 content under elevated CO_2 was associated among other genes with *ISU2* (*AT3G01020*), coding for one of the Fe-S clusters in *Arabidopsis thaliana*, which are known to be essential for photosynthesis and metabolism [21]. Altogether, this demonstrated that genes identified through this approach represent a large and valuable reservoir of candidates to study and to counteract the effect of elevated CO_2 on plant nutrition and ionome content.

To analyze how these genes identified by GWA mapping are regulated by elevated CO_2, we performed RNA-seq from shoots and roots grown under ambient and elevated CO_2.

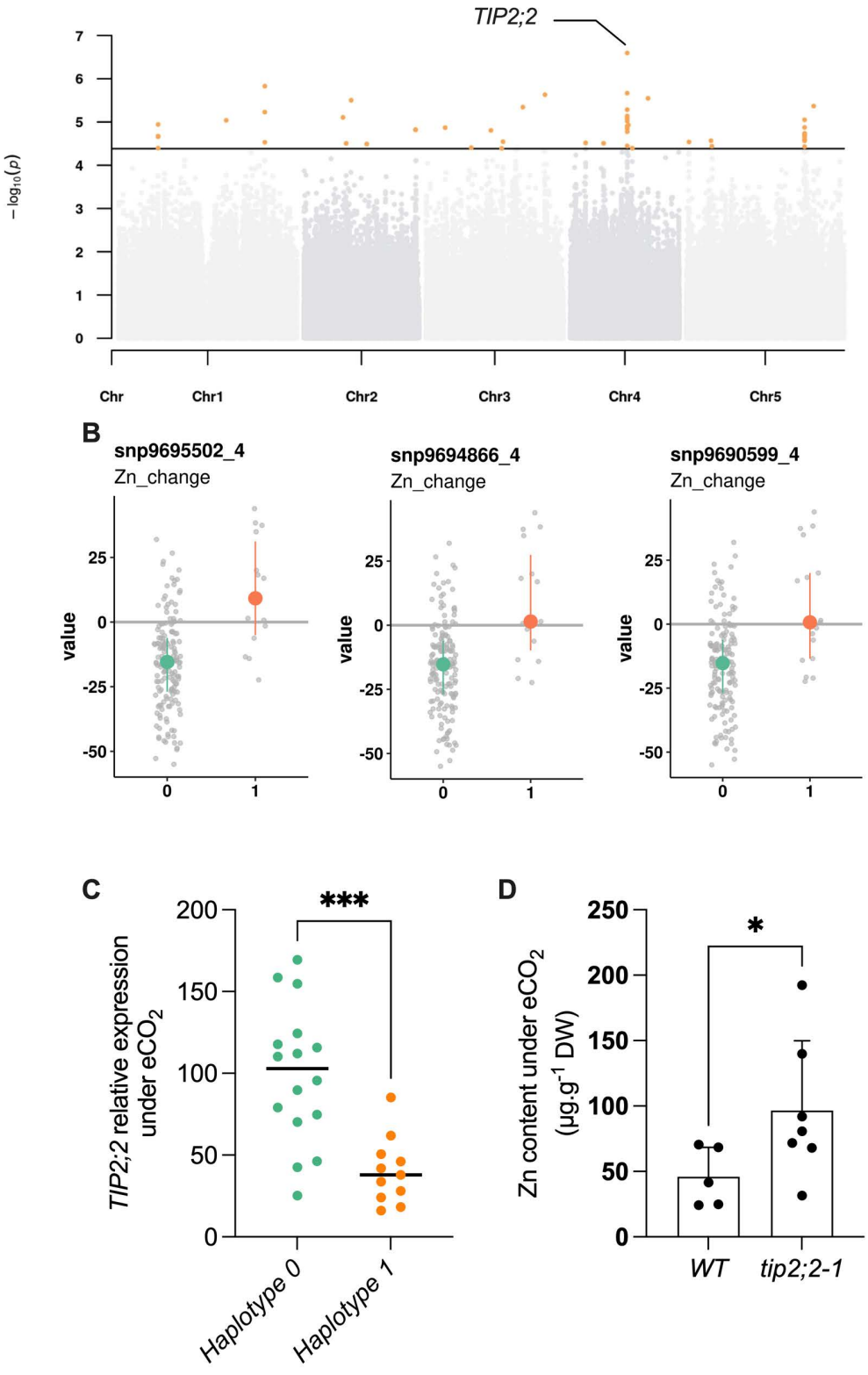

Figure 7: Natural variation of the *TIP2;2* gene is associated with improved responses of Zn content to elevated CO_2. Manhattan plot of the relative change of Zn content between elevated CO2 and ambient CO2 showing the presence of a peak closed to the *TIP2;2* locus. B. Comparison of haplotypes and their relative change of Zn content between elevated CO_2 and ambient CO_2. Three SNPs located at the *TIP2;2* locus are associated to an improvement of Zn content under elevated CO_2 for accessions that possess them (haplotype 1) compared to the rest of the population (haplotype 0). C. Relative expression of *TIP2;2* in the roots under elevated CO_2 for accessions belonging to haplotype 0 or haplotype 1. Relative expression levels were calculated based on *UBQ10* as internal control. Horizontal black line represented the median of each group of haplotypes. ***P < 0,001, unpaired Mann-Whitney test. D. Shoot Zn content under elevated CO_2 for WT (Columbia) and *tip2;2-1* mutant belonging to haplotype 0 or haplotype 1. Data are presented as the mean (with SD) of 5 and 6 biological repeats for the WT and *tip2;2-1*, respectively. *P < 0.05, unpaired Mann-Whitney test.

193 Differentially expressed genes (DEG) associated to the effect of elevated CO_2 were identified
194 from shoots and roots (Suppl. Table 4). We crossed the list of shoots or roots elevated CO_2-
195 DEG with the list of genes identified by GWA mapping for each element, which resulted in a
196 list of 182 genes identified by GWA mapping and differentially regulated by elevated CO_2 in
197 shoot or in roots (Suppl. Table 5), making them strong candidates to be involved in the
198 response of the mineral composition of plants to elevated CO_2. Most of these genes were
199 deregulated by elevated CO_2 in shoot (Fig. 6A, B). In shoot or in roots, these genes mainly
200 showed an association with C-, Mg- or Zn-related traits (Fig. 6A, B). Several of these genes,
201 identified by GWA mapping and whose expression is deregulated in response to high CO_2,
202 were known for their role in nutrient homeostasis. This was the case for the *ASN1* and *DUR3*
203 genes, encoding an asparagine synthase and a urea transporter involved in N metabolism and
204 remobilization, both associated here with a N-related peak of association, and whose
205 expression is modulated by high CO_2 in leaves (Fig. 6C). We also observed in the leaves an
206 interesting profile for several genes related to C metabolism and photosynthesis. This was the
207 case for the *BGP3* gene, involved in chloroplast development, or for the carbonic anhydrase
208 *CA1*, both showing a decreased expression in response to high CO_2 and both associated with
209 a peak in C-related GWA mapping under elevated CO_2 (Fig. 6C). In roots, the gene most
210 deregulated in response to high CO_2 was *AT1G64710*, encoding a GroES-type alcohol
211 dehydrogenase, which interestingly is also deregulated in leaves (Fig. 6D). We also observed
212 in the roots that the expression of the *TIP2;2* gene, associated here with a peak detected for
213 Zn relative change GWA mapping, was deregulated in response to elevated CO_2 (Fig. 6D).
214 To go further, we selected one of the association peaks identified by GWA mapping, and
215 sought to functionally validate the importance of this QTL in response to elevated CO_2, in order
216 to demonstrate the value of our data set and GWA mapping analyses. To do so, we selected

an association peak located on chromosome 4 and associated with Zn relative change (Fig. 7A). More precisely, this association peak displayed the SNPs with the most significant *p*-values and more largely three SNPs that fell into the top 10 SNPs of the trait corresponding to the Zn relative change between ambient and elevated CO_2. The SNPs corresponding to the alternative alleles were associated to an increase of Zn content under elevated CO_2 (Fig. 7B). These SNPs are located very close to the *TIP2;2* (*AT4G17340*) gene, which has been recently characterized as an actor of Zn root-to-shoot translocation [16]. We thus selected a set of accessions from haplotype 0 (reduced Zn content under elevated CO_2) or haplotype 1 (increased Zn content under elevated CO_2), and analyze *TIP2;2* expression in the roots under elevated CO_2. This analysis revealed a haplotype-specific difference in *TIP2;2* expression under elevated CO_2, with accessions from haplotype 1 showing a reduced *TIP2;2* expression in the roots compared to those from haplotype 1 (Fig. 7C), correlated with a higher Zn content in the shoot (Fig. 7B). To validate the effect of *TIP2;2* expression of Zn content under elevated CO_2, we used the *tip2;2-1* knock-out mutant and compared its Zn content under elevated CO_2 to this of the WT. We observed that the *tip2;2-1* mutant line displayed a significant higher Zn content in the shoot under elevated CO_2 compared to the WT, confirming that *TIP2;2* expression determines Zn content under elevated CO_2 (Fig. 7D). Altogether, these results demonstrated that these data sets generated in this study and the associated analyses are a valuable resource to identify genes able to counteract the general negative effect of elevated CO_2 on the mineral composition of plants.

Discussion

The natural variation of ionome response to elevated CO_2 in *Arabidopsis thaliana* displays a high degree of genetic variation

In the present work, we analyzed the diversity of ionome response to elevated CO_2 present in the natural variation of *Arabidopsis thaliana*. In agreement with several other phenotypic traits related to phenology and disease resistance {Brachi, 2013 #1232;Huard-Chauveau, 2013 #1247;Roux, 2022 #1248}, we observed a wide range of responses at complementary geographical scales, from accessions with a ionome strongly negatively affected by high CO_2 to accessions with a ionome benefiting from high CO_2. This confirms for the first time on large and complementary sets of natural genotypes what has been observed by meta-analysis on isolated groups of plants worldwide [2,9]. The global analysis of the distribution of each mineral element studied suggests firstly a trend where the whole ionome would evolve in a unified manner in response to high CO_2, and in an opposite manner to C. This is in line with a number of studies that have proposed that the accumulation of carbohydrates due to the stimulation of photosynthesis by high CO_2 would be the cause of the decrease in plant mineral composition [22-25]. However, the reading of the genetic architecture performed here by a genome-wide association genetics approach suggests that the majority of the genetic mechanisms underlying the negative effect of elevated CO_2 on the ionome are specific to each mineral element. Some specific cases, such as the QTL detected on chromosome 1 and associated with the natural genetic variation of 6 traits among the 20 considered, will certainly deserve a more in-depth analysis.

By clustering globally distributed accessions according to their ionome sensitivity to high CO_2, we were able to observe that the geographic origin of the accessions likely did not determine their response to CO_2. This suggests that inherent genetic factors, more than those due to local adaption, direct the response of plants to elevated CO_2. This seems consistent since the CO_2 elevation applied here to natural *Arabidopsis thaliana* variants does not correspond to any environment experienced by plants yet, at least for several tens of millions of years [26,27].

In this context of brutal and highly impactful environmental change, the presence of cryptic genetic variation often explains the appearance of relatively rapid adaptive mechanisms [28,29]. Although not formally tested here, it would be interesting to examine whether the variation in the ionome in response to elevated CO_2 shows evidence of cryptic variation. In any case, the presence of high phenotypic diversity in these natural populations of *A. thaliana* demonstrates very clearly the possibility of taking advantage of this genetic variation to understand and alleviate the negative response of plant mineral composition to high CO_2.

GWA mapping of ionome variation under elevated CO_2 identified a large number of genes to understand and mitigate the negative effect of high CO_2 on plant mineral composition

In order to understand the genetic mechanisms underlying the effect of high CO_2 on plant mineral composition, and to enable future breeding approaches, we adopted an association genetics approach. This led to the identification of a large number of candidate genes associated to the variation of nutrients under elevated CO_2. Several genes in this list can easily attract attention. In particular, we can note the identification of *ASN1* and *DUR3* genes in two of the loci associated with N content variation under elevated CO_2. *ASN1*, and to a lesser extent *DUR3*, play an important role in the remobilization and the reallocation of N within the plant, and their manipulation can lead to variation in N use efficiency [17,18,30]. This is interesting because for the moment, root N uptake and N assimilation seemed to be the key targets of the negative effect of high CO_2 on plant N content [4,31], but these results suggest that remobilization of N may also be involved. We also identified the *CA1* gene, coding for a carbonic anhydrase, in the vicinity of a QTL associated with C variation under high CO_2. *CA1* is involved in the regulation of stomatal opening by elevated CO_2 [32], and the β carbonic anhydrase family of which *CA1* belongs is involved in the regulation of photosynthetic efficiency, although *CA1* shows no significant effect under standard conditions [33]. It would be

289 therefore interesting to assess the role of *CA1* natural genetic variation under elevated CO_2. If
290 *CA1* regulates the C variation of the ionome under elevated CO_2, this could, according to our
291 observations, significantly influence the global mineral composition of plants. Interestingly,
292 the genes identified by GWA mapping in the ionome response to high CO_2, including those
293 mentioned above, showed substantial variation at the gene expression level. We ended this
294 study with the functional validation of an association peak identified by GWA mapping for the
295 relative change of Zn content between ambient and elevated CO_2. Zn is an essential element
296 for a large number of metabolic processes in humans, and Zn deficiency, found in up to one
297 third of the world's population, leads to severe health problems. We demonstrated that *TIP2;2*
298 gene expression varied in response to CO_2 in a haplotype-specific manner. Consistent with
299 these results, we show that manipulating *TIP2;2* expression with a knock-out mutant can
300 modulate the Zn loss observed under high CO_2. A recent study demonstrated that TIP2;2 was
301 responsible for Zn retention in the roots {Wang, 2022 #1177}. It therefore seems consistent
302 that natural accessions with the lowest expression levels of this gene are those with the
303 highest Zn content in aerial parts, due to low retention in their roots. This example illustrates
304 the potential of the resource we have generated here towards the development of biofortified
305 plants. The development of biofortified plants represents a considerable challenge in view of
306 the current problems of malnutrition on a global scale, and this challenge becomes even more
307 important in a context of rising atmospheric CO_2 [34]. This reservoir of data and genes will
308 certainly contribute to the understanding of the mechanisms underlying the general negative
309 effect of CO_2 on mineral composition, and to the development of crop plants adapted to
310 forthcoming high-CO_2 climate.
311
312 **Methods**

Data and code availability

Data and R notebooks containing the analyses performed in this article can be found at https://src.koda.cnrs.fr/groups/ipsim/sirene-team. RNA-seq data generated for this study are available at https://www.ebi.ac.uk/biostudies/arrayexpress/studies using the accession no xxx.

Plant Material

A subset of the REGMAP panel, the LANGUEDOC panel and the TOU-A panel were used in this study. These populations were previously described here {Brachi, 2013 #1232;Frachon, 2017 #1249;Horton, 2012 #1231}. These populations were grown on Jiffy-7 peat pellets (Jiffy Products International, NL) under ambient (~420 ppm) or elevated (900 ppm) CO_2 in the growth chambers of the Microcosms experimental platform at the Montpellier European Ecotron CNRS. Growth conditions were 6-h/22-h light (22°C) / dark (20°) photoperiod, with 200 µmol m^{-2} s^{-1} light intensity and 65% of hygrometry. Plants were watered twice a week with a growth solution containing KH_2PO_4 1 mM, $MgSO_4$ 1 mM, K_2SO_4 250 µM, $CaCl_2$ 250 µM, Na-Fe-EDTA 100 µM, KNO_3 10 mM, KCl 50 µM, H_3BO_3 30 µM, $MnSO_4$ 5 µM, $ZnSO_4$ 1 µM, $CuSO_4$ 1 µM, $(NH_4)_6Mo_7O_{24}$ 0,1 µM, as described by [35]. The entire rosettes were collected three weeks after sowing. The *tip2;2-1* mutant line corresponds to the *SALK_152463* allele [16].

Ionome analysis

From 3 to 5 replicates per accession were used for each ionome analysis. Total C and N content was obtained from dried shoot tissue using an Elementar Pyrocube analyzer. Cu, Fe, Mg, Mn, Na and Zn content was obtained from dry shoot tissue mixed with 750 µl of nitric acid (65% [v/v]) and 250 µl of hydrogen peroxide (30% [v/v]). After one night at room temperature, samples were mineralized at 85°C during 24 hours. Once mineralized, 4 ml of milliQ water was

added to each sample. Mineral contents present in the samples were then measured by microwave plasma atomic emission spectroscopy (MP-AES, Agilent Technologies).

Removal of outlier observations

Prior to GWAS and multivariate analyses such as PCA or clustering, mineral composition measures were pre-processed to remove technical outliers. For a given element and CO_2 condition, the values positioned more than 5 median absolute deviations away from the median were removed from the dataset.

PCA and Clustering

Principal Component Analysis was performed using the R *ade4* package after the prior scaling of the variables to a z-score. Clustering of the REGMAP panel based on the relative changes of the mineral composition of each accession has been done using a k-means clustering with the R *kmeans* function. For this step, the variables were also scaled to a z-score. The number of clusters in the k-means algorithm was chosen by the elbow method on the criteria of cluster homogeneity (within-sum of squares).

GWAs

Genome-Wide Association mapping was performed using the R *statgenGWAS* package. Genotype data was prepared using the *codeMarkers* function, removing duplicated SNPs and filtering for a minimum allele relative frequency of 0.04. Associations were performed by the *runSingleTraitGwas* function, that implements the EMMA algorithm. Population structure was modeled via a kinship matrix built from the Astle method. Manhattan plots were drawn using the *manPlotFast* function of the *ramwas* R package.

RNA-seq experiments

Plants were grown in hydroponics to have access to the roots in addition to the shoot, as previously described in [4]. Shoot or root from 5 plants were pooled into one biological replicate,

flash frozen in liquid nitrogen, and stored at -80◦C. RNA of three biological replicates were extracted from shoot or root tissues using Direct-zol RNA Miniprep (Zymo Research, CA, USA), according to the manufacturer recommendations. RNA-sequencing libraries were done from shoot or root total RNA using standard RNA-Seq protocol method (Poly-A selection for mRNA species) by the Novogene company. RNA-sequencing was performed using Illumina technology on a NovaSeq6000 system providing PE150 reads. The quality control and adapter trimming of raw paired-end fastq files was done with *fastp* and its default parameters. Mapping to the TAIR10 reference genome was performed with STAR, and using the following options:

--outSAMtype BAM SortedByCoordinate

--outFilterMismatchNmax 1

--outFilterMismatchNoverLmax 0.15

--alignIntronMin 30

--alignIntronMax 5000

Quantification of the bam files against the TAIR10 GFF3 annotation file was done using *htseq-count* with options:

-f bam --type gene -r pos

--idattr=Name --stranded=no

Normalization and differential expression were performed using *DIANE* R package [36], with no fold change constraint, and an adjusted p-value threshold (FDR) of 0.05. Lowly expressed genes with an average value across conditions under 25 reads were excluded from the analysis.

Quantitative real-time PCR

Plants were grown in hydroponics to have access to the roots, as previously described in [4]. Root tissue from 5 plants were pooled into one biological replicate, flash frozen in liquid nitrogen, and stored at -80◦C. RNA were extracted from shoot or root tissues using TRIZOL (Invitrogen, USA), according to the manufacturer recommendations, and DNAse treated using RQ1 (Promega, USA). Reverse transcription was achieved from 1 μg of total RNA with M-MLV reverse transcriptase (RNase H minus, Point Mutant, Promega, USA) using an anchored oligo(dT)20 primer. Accumulation of transcripts was measured by qRT-PCR (LightCycler 480, Roche Diagnostics, USA) using the SYBR Premix Ex TaqTM (TaKaRa, Japan). Gene expression was normalized using *UBQ10* and *ACT2* as internal standards. Results are presented as the expression relative to *UBQ10*. Sequences of primers used in RT-qPCR for gene expression analysis are listed in Supplemental Table 6.

Acknowledgments

This work was supported by the I-Site Montpellier Université d'Excellence (MUSE; project ECO2THREATS), the CNRS through the Mission for Transversal and Interdisciplinary Initiatives (MITI) 80 PRIME program, and the Plant Biology and Breeding department of INRAE. O.C. was recipient of a PhD fellowship from the CNRS. T.M. was recipient of a PhD fellowship from INRAE and Région Occitanie. We thank Jiping Liu from Cornell University for the gift of *tip2;2-1* mutant line. This study benefited from the CNRS human and technical resources allocated to the Ecotron Research Infrastructure and from the state allocation "Investissement d'Avenir" AnaEE France ANR-11-INBS-0001.

References

1 Gojon, A., Cassan, O., Bach, L., Lejay, L. & Martin, A. The decline of plant mineral nutrition under rising CO2: physiological and molecular aspects of a bad deal. *Trends in Plant Science* **28**, 185-198 (2023). https://doi.org:10.1016/j.tplants.2022.09.002

2 Loladze, I. Hidden shift of the ionome of plants exposed to elevated CO(2)depletes minerals at the base of human nutrition. *Elife* **3**, e02245 (2014). https://doi.org:10.7554/eLife.02245

3 Bouain, N. *et al.* Plant growth stimulation by high CO2 depends on phosphorus homeostasis in chloroplasts. *Curr Biol* (2022). https://doi.org:10.1016/j.cub.2022.08.032

4 Cassan, O. *et al.* A gene regulatory network in Arabidopsis roots reveals features and regulators of the plant response to elevated CO(2). *New Phytol* (2023). https://doi.org:10.1111/nph.18788

5 Sun, P. *et al.* Countering elevated CO2 induced Fe and Zn reduction in Arabidopsis seeds. *New Phytol* **235**, 1796-1806 (2022). https://doi.org:10.1111/nph.18290

6 Umnajkitikorn, K., Sade, N., Rubio Wilhelmi, M. D. M., Gilbert, M. E. & Blumwald, E. Silencing of OsCV (chloroplast vesiculation) maintained photorespiration and N assimilation in rice plants grown under elevated CO(2). *Plant Cell Environ* **43**, 920-933 (2020). https://doi.org:10.1111/pce.13723

7 Yang, A., Li, Q., Chen, L. & Zhang, W.-H. A rice small GTPase, Rab6a, is involved in the regulation of grain yield and iron nutrition in response to CO2 enrichment. *Journal of Experimental Botany* **71**, 5680-5688 (2020). https://doi.org:10.1093/jxb/eraa279

8 Marcos-Barbero, E. L., Pérez, P., Martínez-Carrasco, R., Arellano, J. B. & Morcuende, R. Screening for Higher Grain Yield and Biomass among Sixty Bread Wheat Genotypes Grown under Elevated CO2 and High-Temperature Conditions. *Plants* **10**, 1596 (2021).

9 Myers, S. S. *et al.* Increasing CO2 threatens human nutrition. *Nature* **510**, 139-142 (2014). https://doi.org:10.1038/nature13179

10 Zhu, C. *et al.* Carbon dioxide (CO2) levels this century will alter the protein, micronutrients, and vitamin content of rice grains with potential health consequences for the poorest rice-dependent countries. *Sci Adv* **4**, eaaq1012 (2018). https://doi.org:10.1126/sciadv.aaq1012

11 Arouisse, B., Korte, A., van Eeuwijk, F. & Kruijer, W. Imputation of 3 million SNPs in the Arabidopsis regional mapping population. *The Plant Journal* **102**, 872-882 (2020). https://doi.org:https://doi.org/10.1111/tpj.14659

12 Baxter, I. *et al.* A Coastal Cline in Sodium Accumulation in Arabidopsis thaliana Is Driven by Natural Variation of the Sodium Transporter AtHKT1;1. *PLOS Genetics* **6**, e1001193 (2010). https://doi.org:10.1371/journal.pgen.1001193

13 North, K. A., Ehlting, B., Koprivova, A., Rennenberg, H. & Kopriva, S. Natural variation in Arabidopsis adaptation to growth at low nitrogen conditions. *Plant Physiology and Biochemistry* **47**, 912-918 (2009). https://doi.org:https://doi.org/10.1016/j.plaphy.2009.06.009

14 Kim, S. *et al.* Recombination and linkage disequilibrium in Arabidopsis thaliana. *Nature Genetics* **39**, 1151-1155 (2007). https://doi.org:10.1038/ng2115

15 Katz, E. *et al.* Genetic variation underlying differential ammonium and nitrate responses in Arabidopsis thaliana. *The Plant Cell* **34**, 4696-4713 (2022). https://doi.org:10.1093/plcell/koac279

16 Wang, Y. *et al.* AtTIP2;2 facilitates resistance to zinc toxicity via promoting zinc immobilization in the root and limiting root-to-shoot zinc translocation in Arabidopsis thaliana. *Ecotoxicology and Environmental Safety* **233**, 113333 (2022). https://doi.org:https://doi.org/10.1016/j.ecoenv.2022.113333

17 Gaufichon, L. *et al.* ASN1-encoded asparagine synthetase in floral organs contributes to nitrogen filling in Arabidopsis seeds. *The Plant Journal* **91**, 371-393 (2017). https://doi.org:https://doi.org/10.1111/tpj.13567

18 Lam, H.-M. *et al.* Overexpression of the ASN1 Gene Enhances Nitrogen Status in Seeds of Arabidopsis. *Plant Physiology* **132**, 926-935 (2003). https://doi.org:10.1104/pp.103.020123

19 Li, Y. *et al.* Combined analyses of translatome and transcriptome in Arabidopsis reveal new players responding to magnesium deficiency. *Journal of integrative plant biology* **63**, 2075-2092 (2021). https://doi.org:https://doi.org/10.1111/jipb.13169

20 Brun, A. *et al.* MCO1 and MCO3, two putative ascorbate oxidases with ferroxidase activity, new candidates for the regulation of apoplastic iron excess in Arabidopsis. *Plant Direct* **6**, e463 (2022). https://doi.org:10.1002/pld3.463

21 Balk, J. & Schaedler, T. A. Iron cofactor assembly in plants. *Annu Rev Plant Biol* **65**, 125-153 (2014). https://doi.org:10.1146/annurev-arplant-050213-035759

22 Ainsworth, E. A. & Long, S. P. What have we learned from 15 years of free-air CO2 enrichment (FACE)? A meta-analytic review of the responses of photosynthesis, canopy properties and plant production to rising CO2. *New Phytol* **165**, 351-371 (2005). https://doi.org:10.1111/j.1469-8137.2004.01224.x

474 23 Dusenge, M. E., Duarte, A. G. & Way, D. A. Plant carbon metabolism and climate
475 change: elevated CO2 and temperature impacts on photosynthesis, photorespiration
476 and respiration. *New Phytol* **221**, 32-49 (2019). https://doi.org:10.1111/nph.15283
477 24 Tausz-Posch, S., Tausz, M. & Bourgault, M. Elevated [CO2] effects on crops: Advances
478 in understanding acclimation, nitrogen dynamics and interactions with drought and
479 other organisms. *Plant Biol (Stuttg)* **22 Suppl 1**, 38-51 (2020).
480 https://doi.org:10.1111/plb.12994
481 25 Thompson, M., Gamage, D., Hirotsu, N., Martin, A. & Seneweera, S. Effects of Elevated
482 Carbon Dioxide on Photosynthesis and Carbon Partitioning: A Perspective on Root
483 Sugar Sensing and Hormonal Crosstalk. *Front Physiol* **8**, 578 (2017).
484 https://doi.org:10.3389/fphys.2017.00578
485 26 Luthi, D. *et al.* High-resolution carbon dioxide concentration record 650,000-800,000
486 years before present. *Nature* **453**, 379-382 (2008).
487 https://doi.org:10.1038/nature06949
488 27 Pearson, P. N. & Palmer, M. R. Atmospheric carbon dioxide concentrations over the
489 past 60 million years. *Nature* **406**, 695-699 (2000). https://doi.org:10.1038/35021000
490 28 Cortés, A. J. & López-Hernández, F. Harnessing Crop Wild Diversity for Climate Change
491 Adaptation. *Genes* **12**, 783 (2021).
492 29 Pauls, S. U., Nowak, C., Balint, M. & Pfenninger, M. The impact of global climate change
493 on genetic diversity within populations and species. *Mol Ecol* **22**, 925-946 (2013).
494 https://doi.org:10.1111/mec.12152
495 30 Bohner, A., Kojima, S., Hajirezaei, M., Melzer, M. & von Wirén, N. Urea retranslocation
496 from senescing Arabidopsis leaves is promoted by DUR3-mediated urea retrieval from

497 leaf apoplast. *The Plant Journal* **81**, 377-387 (2015).
498 https://doi.org:https://doi.org/10.1111/tpj.12740

499 31 Bloom, A. J., Burger, M., Rubio Asensio, J. S. & Cousins, A. B. Carbon dioxide enrichment
500 inhibits nitrate assimilation in wheat and Arabidopsis. *Science* **328**, 899-903 (2010).
501 https://doi.org:10.1126/science.1186440

502 32 Hu, H. *et al.* Distinct Cellular Locations of Carbonic Anhydrases Mediate Carbon Dioxide
503 Control of Stomatal Movements *Plant Physiology* **169**, 1168-1178 (2015).
504 https://doi.org:10.1104/pp.15.00646

505 33 Sharma, N. *et al.* Arabidopsis stromal carbonic anhydrases exhibit non-overlapping
506 roles in photosynthetic efficiency and development. *Plant J* **n/a** (2023).
507 https://doi.org:10.1111/tpj.16231

508 34 Shahzad, Z. & Rouached, H. Protecting plant nutrition from the effects of climate
509 change. *Curr Biol* **32**, R725-R727 (2022). https://doi.org:10.1016/j.cub.2022.05.056

510 35 Gansel, X., Munos, S., Tillard, P. & Gojon, A. Differential regulation of the NO3- and
511 NH4+ transporter genes AtNrt2.1 and AtAmt1.1 in Arabidopsis: relation with long-
512 distance and local controls by N status of the plant. *Plant J* **26**, 143-155 (2001).

513 36 Cassan, O., Lebre, S. & Martin, A. Inferring and analyzing gene regulatory networks
514 from multi-factorial expression data: a complete and interactive suite. *BMC Genomics*
515 **22**, 387 (2021). https://doi.org:10.1186/s12864-021-07659-2

516

Figure legends :

Figure 1: Elevated CO_2 negatively impacts the ionome content at the population-scale level in *Arabidopsis thaliana*. A. Representation of the experimental design used in this study. The content of eight mineral elements was assessed for around 600 *Arabidopsis thaliana* accessions coming from the REGMAP (B), LANGUEDOC (C) and TOU-A (D) populations. Each dot represents the value of the content of a mineral element for one accession (yellow: ambient CO_2 (aCO_2, ~420 ppm), blue: elevated CO_2 (eCO_2, 900 ppm). N (% of dry weight), Fe ($\mu g.g^{-1}$ dry weight), Zn ($\mu g.g^{-1}$ dry weight), Cu ($\mu g.g^{-1}$ dry weight), Mg ($\mu g.g^{-1}$ dry weight), Mn ($\mu g.g^{-1}$ dry weight), Na ($\mu g.g^{-1}$ dry weight), C (% of dry weight). Asterisks indicate significant differences (Paired Wilcoxson test; *, $P < 0.05$; **, $P < 0.005$; ***, $P < 0.0005$). ns; not significant.

Figure 2: Elevated CO_2 leads to high phenotypic diversity of ionome response in *Arabidopsis thaliana*. Distributions of the relative change (%) of the content of 8 mineral elements between elevated CO_2 and ambient CO_2, in each population (A: REGMAP, B: LANGUEDOC, C: TOU-A). Each dot represents the value of the relative change of the content a mineral element for one accession. The name of the element appears in bold if the mean of the element in elevated CO_2 is significantly different from the mean of the element in ambient CO_2 (Paired wilcoxon test, significance threshold of 0.05).

Figure 3: Elevated CO_2 results in a general pattern of ionome variation common to most accessions constituting natural populations of *Arabidopsis thaliana*. Principal Component Analysis (PCA) was performed using the variation of each element in response to elevated CO_2.

A. Natural accessions were positioned on the PCA and colored based on population. B. Contribution of each element to the PCA axis.

Figure 4: Variation in the response of the ionome to elevated CO_2 identifies contrasting subpopulations inside the REGMAP panel. K-means clustering was performed in the REGMAP accessions to identify different subpopulations. Each accession is represented by a dot, connected by a line between each element. Cluster 1:65 accessions. Cluster 2: 25 accessions. Cluster 3: 69 accessions.

Figure 5: Genetic architecture of the response of the ionome to elevated CO_2 in the REGMAP panel of *Arabidopsis thaliana.* A. Manhattan plots for the content of eight mineral elements under elevated CO_2, or for the relative change of the content of mineral elements between elevated CO_2 and ambient CO_2. For each Manhattan plot, SNPs with the 50 most significant P-value, located above the horizontal line, are colored. Bar plots showing the number of SNPs identified by GWAs for traits under elevated CO_2 (B) or for the relative change of the content of mineral elements between elevated CO_2 and ambient CO_2 (C) that are unique to one element or shared between 2 or 3 traits.

Figure 6: Identification of genes detected by GWA mapping and differentially regulated by elevated CO_2. Intersection between elevated CO_2-DEG in shoot (A) or root (B) and genes identified by GWA mapping. UpSet plots display the number of elevated CO_2-DEG that are associated to a locus identified for the content or the relative change of one or several mineral elements under elevated CO_2. Illustration of the pattern of elevated CO_2-DEG in shoot (C) or root (D) also identified by GWA mapping.

Figure 7: Natural variation of the *TIP2;2* gene is associated with improved responses of Zn content to elevated CO_2. Manhattan plot of the relative change of Zn content between elevated CO2 and ambient CO2 showing the presence of a peak closed to the *TIP2;2* locus. B. Comparison of haplotypes and their relative change of Zn content between elevated CO_2 and ambient CO_2. Three SNPs located at the *TIP2;2* locus are associated to an improvement of Zn content under elevated CO_2 for accessions that possess them (haplotype 1) compared to the rest of the population (haplotype 0). C. Relative expression of *TIP2;2* in the roots under elevated CO_2 for accessions belonging to haplotype 0 or haplotype 1. Relative expression levels were calculated based on *UBQ10* as internal control. Horizontal black line represented the median of each group of haplotypes. ***P < 0,001, unpaired Mann-Whitney test. D. Shoot Zn content under elevated CO_2 for WT (Columbia) and *tip2;2-1* mutant belonging to haplotype 0 or haplotype 1. Data are presented as the mean (with SD) of 5 and 6 biological repeats for the WT and *tip2;2-1*, respectively. *P < 0.05, unpaired Mann-Whitney test.